Productivity of the Ocean: Present and Past
eds. W.H. Berger, V.S. Smetacek and G. Wefer, pp. 117–137
John Wiley & Sons Limited

Regional Extremes in Particulate Matter Composition and Flux: Effects on the Chemistry of the Ocean Interior

J.K.B. Bishop

Lamont-Doherty Geological Observatory
Columbia University
Palisades, NY 10964, U.S.A.

Abstract. This paper reviews what is known about productivity patterns and vertical flux of organic carbon, opal, and carbonate in the biologically active upper 1000–2000 m of the ocean. Our ability to model particulate carbon flux as a function of depth and primary productivity is much worse than our ability to model particulate carbon flux and regeneration rates as a function of depth once the particulate carbon flux at 100 m is known. A major term missing in equations linking primary production and particle flux appears to be one describing the consumption of particles by macrozooplankton and other large animals.

Simple empirically derived rules based on abundances and chemistry of suspended matter and the mean temperature of the upper 200 m appear sufficient to map the first-order global patterns of production of organic carbon, carbonate, opal, and barium. These may be applicable to both past and present oceanographic conditions.

INTRODUCTION

The vertical distribution of carbon species in the ocean is controlled mainly by biologically mediated processes—photosynthesis, feeding, respiration, and decay—which collectively make up the "biological pump" (Fig. 1). The pump intake is located in surface waters where carbon is transformed from dissolved inorganic forms to particulate organic matter by phytoplankton in the presence of light and nutrients. The impeller—or active mechanism in the pump—is the feeding activity of zooplankton and fish which consume the phytoplankton-produced carbon and package a fraction of it in fecal material which sinks into the deep sea at hundreds of meters per day. Daily vertical migrations of zooplankton and nekton may be an additional way for carbon to be transported from the surface to the deep sea (Angel, this

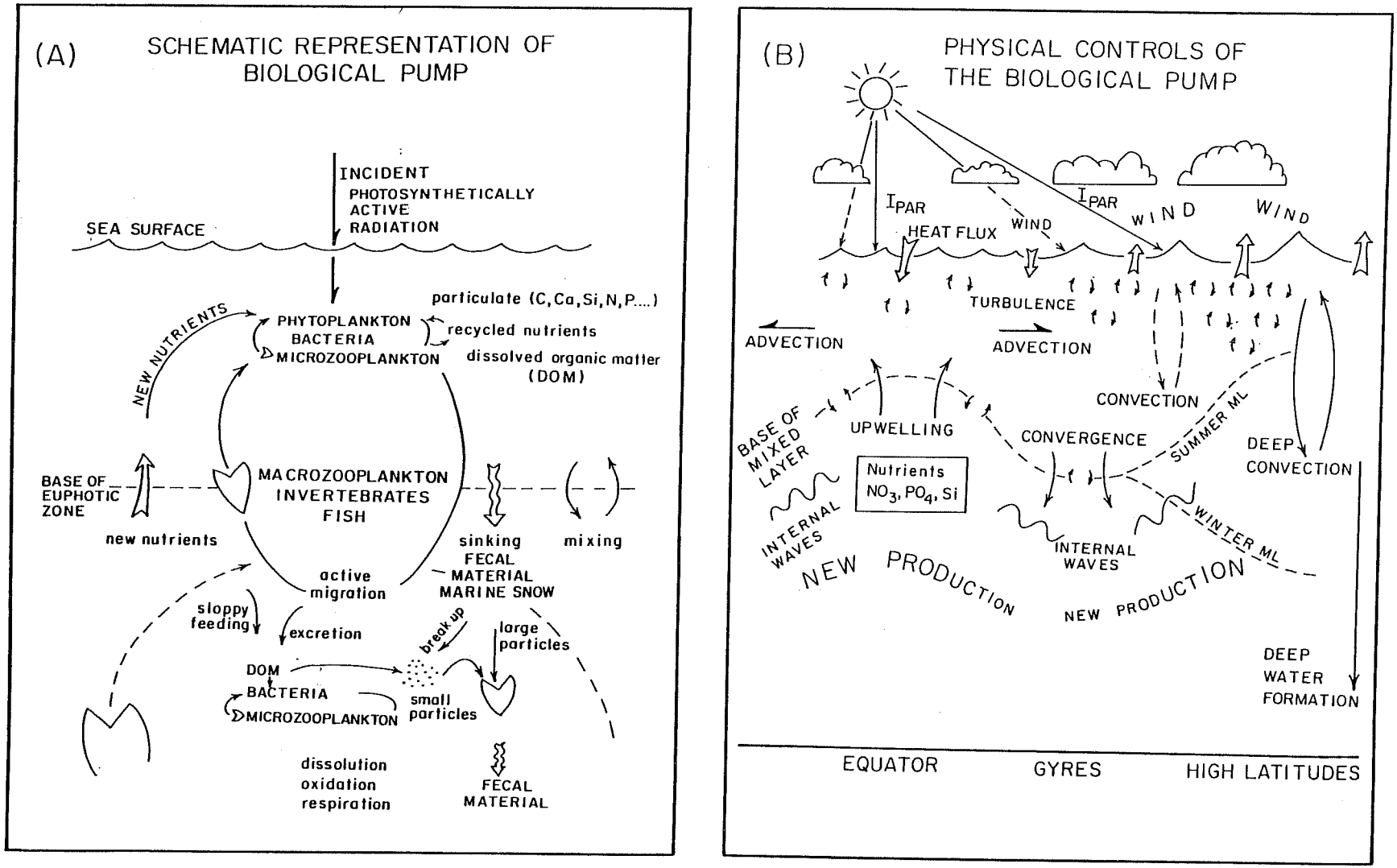

Fig. 1—Schematic representation of the biological pump (A) and of physical processes controlling the biological pump (B).

volume). In some oceanic regions, sinking aggregations of phytoplankton may also contribute to the flux. The discharge of the pump occurs deeper where the organic matter in fecal material, animal tissue, or excreted dissolved organic matter (DOM) is oxidized back to dissolved inorganic carbon species (largely through the activities of bacteria and microzooplankton). The pump forms a major pathway for carbon to move from surface waters into the deep sea. The other pathway for carbon to enter the deep ocean is in polar regions where surface waters are subducted to form deep water. Therefore, the operation and efficiency of the "biological pump" may be an important factor in the removal of anthropogenic CO_2 from the atmosphere to the ocean. The pump is of importance not only to the global carbon cycle but to the cycles of many other chemical species (Ca, Si, N, P, and trace metals such as Ba, Cd, Ni, Zn, and others).

Operation of the pump depends on two dominant processes: (*a*) photosynthesis, which depends on light and nutrient availability in the near surface waters, and (*b*) zooplankton feeding activity. At the base of the euphotic zone, the downward flux (or export flux) of organic matter must, on the whole, be balanced by the upward supply of nutrients (particularly NO_3^-). This is the familiar concept of "new production" (Dugdale and Goering 1967; Eppley, this volume). The fraction of photosynthesis supported by NH_4^+ and urea is recycled within the euphotic zone. A frequently used assumption is that particle flux through the base of the euphotic zone is the sole balancing term for new production and that this balance is achieved on time scales of days. In some oceanic regions, active transport by migrating animals and deep convective mixing may contribute significantly to the flux of organic matter through the base of the euphotic zone, and alter the time scales over which new production is in balance with export flux.

A schematic view of the biological pump and the physical and biological processes which govern its operation is represented in Fig. 1. The global field of photosynthetically active radiation (PAR, about 50% of incident solar radiation)—the primary driving force for the biological pump—varies with latitude, season, and cloudiness. Nutrient supply to the euphotic zone is governed by turbulent, convective, and advective motions of the water column, which are also predominantly forced from above, and by the nutrient concentrations in subsurface waters. Significant effort has been invested in the development of detailed models incorporating the effects of biological and physical processes on the biological pump (e.g., Kamykowski 1987; Toggweiler, this volume) and, in spite of significant progress, they are still in the developmental stages.

The purpose of this paper is to review some of what is known and not known about the biological pump in the upper 1000–2000 m and to test and suggest some simple relationships which can be used as a basis for modeling the cycles of carbon, Si, alkalinity, and Ba—all of which have well-

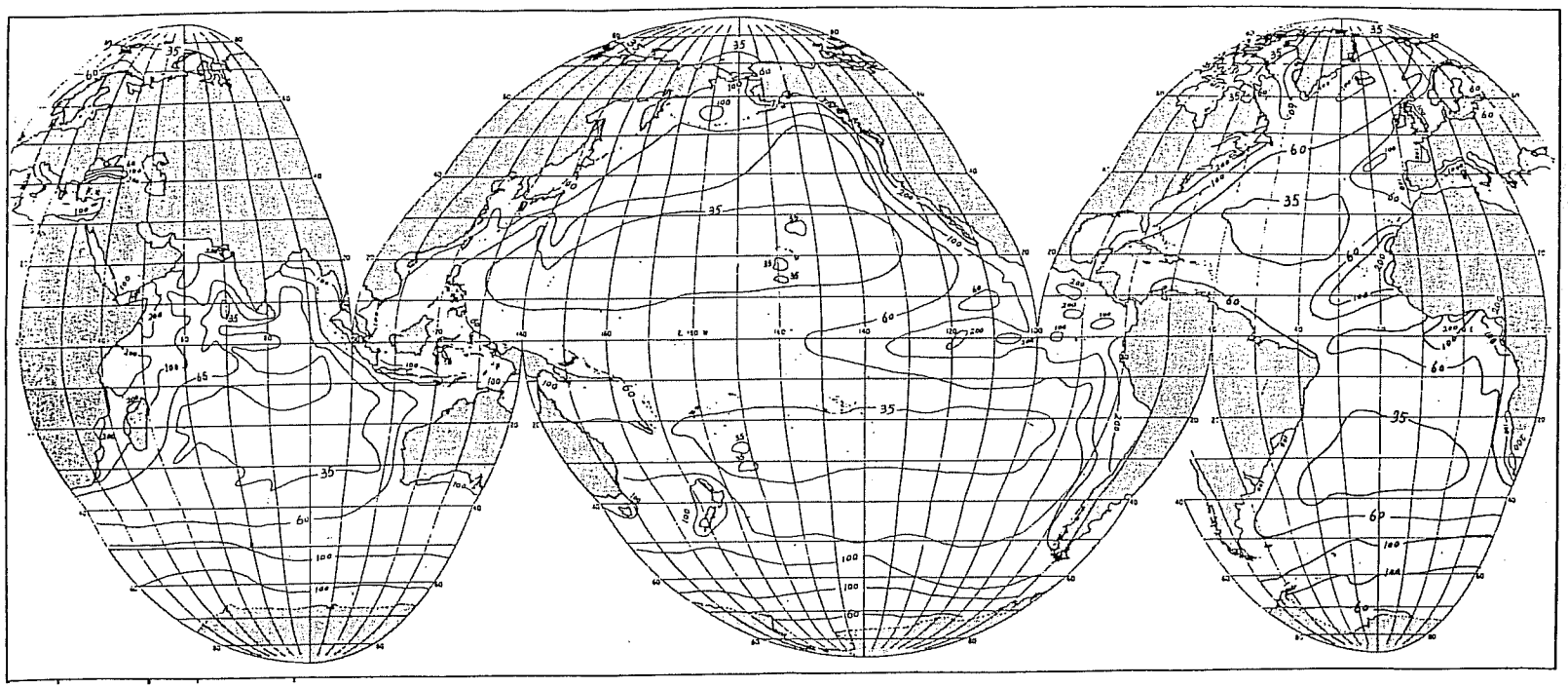

Fig. 2—Average carbon primary productivity of the ocean as compiled from the literature (from Berger et al. 1987).

characterized dissolved distributions in the world's ocean. Some derived relationships may appear to be gross extrapolations but they may permit us to understand the first-order patterns of ocean productivity of these elements past and present. We are presently very far from the goal of understanding the effects of sinking and suspended matter on the chemistry of the ocean interior.

CARBON

Global Patterns of Primary Production

Much of our present understanding of global primary production (the feed for the biological pump) has relied on measurements of primary production measured by the ^{14}C incubation technique and on larger data sets describing the nutrient fields in the upper water column (e.g., Koblentz-Mishke et al. 1970). Figure 2 is a map of mean annual primary productivity constructed by Berger et al. (1987). Large gaps in station coverage exist south of 30°S in all oceans and surprisingly few measurements (1-10 per 10 degree square) were available for large regions of the North Atlantic. Nevertheless, Berger and co-workers constructed a set of simple rules relating primary production to available nutrients (PO_4^{3-} at 100 m), light (latitude), and proximity to continental margins which enabled them to fill in the gaps of station coverage. Whether or not their maps are accurate in detail, they are certainly valuable for understanding patterns of carbon fixation in the ocean and can serve as a starting point for estimates of organic matter delivery to the deep sea. Particulate matter residence times based on $^{234}Th/^{238}U$ are highly correlated with values of primary productivity derived largely from old ^{14}C data and with particle flux rates estimated using sediment traps (Bruland and Coale 1986). The calculated residence times are not as well correlated with contemporary measurements of primary productivity (Bruland, personal communication). Consequently, the patterns shown in the figure may more closely represent that of export production.

Parameterizations of Vertical Carbon Flux

Berger et al. (1987) reviewed sediment trap data published prior to 1986 and various formulations which might be used to model particulate organic carbon flux as a function of depth using maps of primary production. Approximately twice as much data are available now (211 points), mostly for the upper 2000 m from estimates of vertical carbon transport determined by short-term deployments of drifting sediment traps (e.g., Martin et al. 1987) and by large volume *in situ* filtration (LVFS; e.g., Bishop et al. 1987). The new data mostly come from the eastern Pacific but some come from

the N.W. Atlantic, including environments influenced by deep convective mixing, persistent upwelling, and late season destratification. The problems associated with sediment trap and LVFS estimates of vertical flux will not be reviewed here since they are adequately described in the literature. The point of this exercise is to show that empirically derived relationships for vertical carbon flux as a function of primary productivity and depth show errors greatly exceeding the factor of 2–3 uncertainty of the data. Significant improvement may be possible by adding a zooplankton consumer term.

Eight empirical relationships describing particle flux (J: units g C m^{-2} y^{-1}) are summarized by Equations 1–8 and are evaluated in Figs. 3a and b.

$J = PP/(0.024z + 0.21)$	Suess (1980)	(1)
$J = 0.409PP^{1.41}/z^{0.628}$	Betzer, Showers et al. (1984)	(2)
$J = 20PP/z$	Berger et al. (1987), simple fit to data <1000 m	(3)
$J = 6.3PP/z^{0.8}$	Berger et al. (1987), best fit to data <1000 m	(4)
$J = 17PP/z + PP/100$	Berger et al. (1987), refractory carbon model	(5)
$J = 9PP/z + 0.7PP/z^{0.5}$	Berger et al. (1987), good fit all data	(6)
$J = 1.286PP/z^{0.734}$	Pace et al. (1987), vertex: N.E. Pacific	(7)
$J = J_{100}/((z/100)^{0.858})$	Martin et al. (1987), vertex: open ocean	(8)

The first 7 empirical relationships tested depend only on primary production (PP), and depth (z), and equations 5, 6, and 7 appear least biased and better behaved compared with equations 1–4; however, it is difficult to prefer any one of the three. Martin et al. (1987) showed that if the particle flux at 100 m (J_{100}) was known, much better estimates of particle flux to deeper waters could be made. The test of this relationship (Eq. 8) using available data did show significant improvement (Fig. 3b). The major implication is that we must be missing an additional term in the equations which use primary production and depth to predict flux. Simply restated, if we had a global map of particle flux at 100 m, then much better estimates of particle flux and regeneration in deeper waters could be made.

Even using the Martin et al. (1987) relationship, some estimated fluxes fall on the high and low sides of the "measured" flux by as much as an order of magnitude. Martin et al. (1987) showed that the depth exponent used in Eq. 8 was as low as 0.3 for their coastal data and as high as 1.0. If some LVFS data from the Warm Core Rings experiment are included, then the upper limit of the exponent may be as high as 1.5. Is the range of the exponent a consequence of differences between zooplankton feeding demand and particulate matter production in the different environments sampled? The answer is probably yes and evidence to support this is found

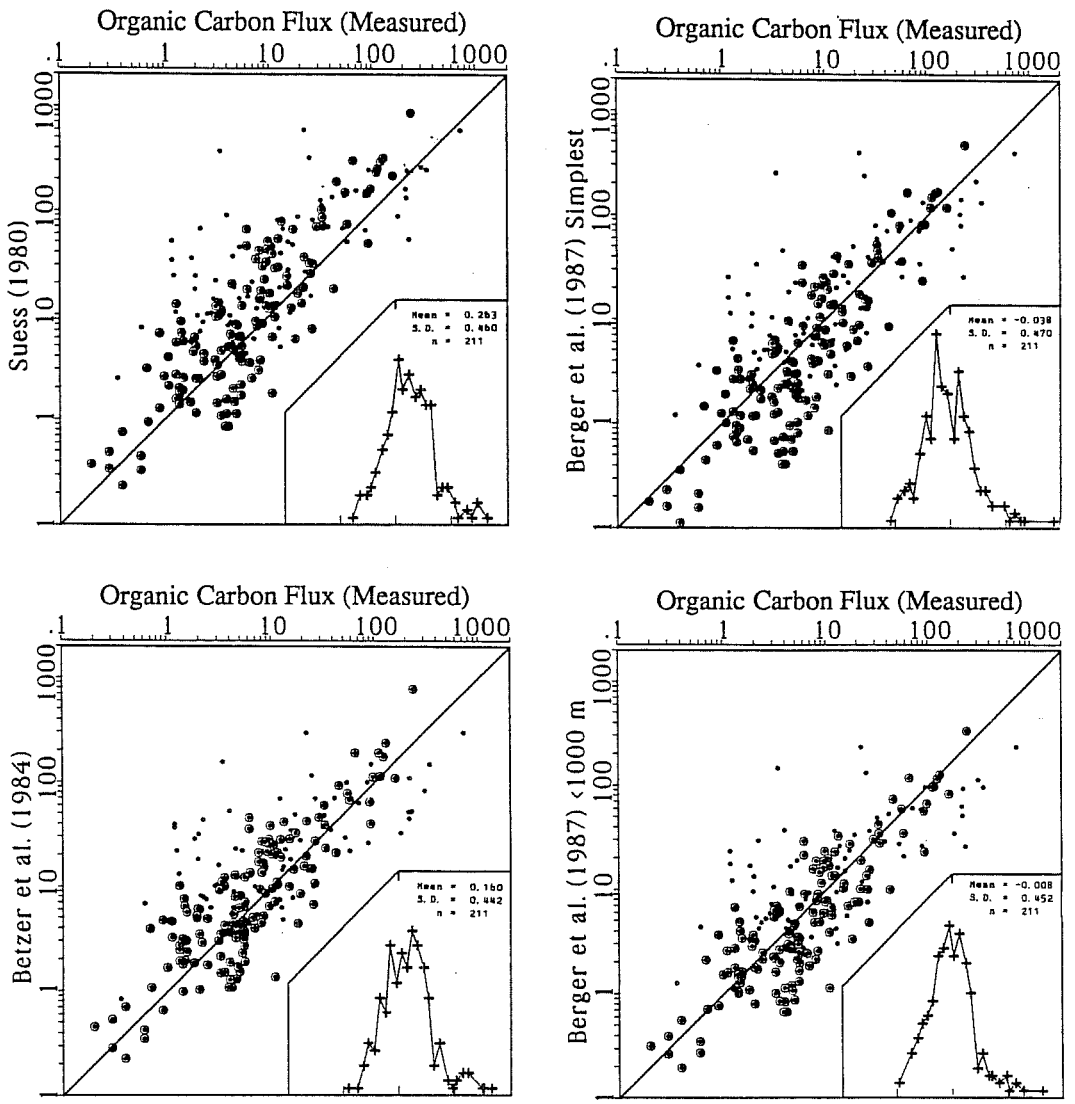

Fig. 3*a*—Test of empirical relationships (1–4) for carbon flux as a function of primary production and depth. Small symbols (•) denote carbon flux data from LVFS observations, large symbols (◉) denote carbon flux data from sediment trap observations. The inset is a frequency histogram of the ratio of empirically derived carbon flux to measured carbon flux on a log scale from 0.01 to 100. The y axis of the inset is the number of observations on a scale of 0–30.

in Bishop et al. (1987), who found a consistent relationship between particle flux gradient and zooplankton biomass in the Panama Basin. Unfortunately, few data on distributions of zooplankton biomass have been gathered in conjunction with particle flux studies. Simple rules governing the global distributions of zooplankton (and fish) and their impact on particle flux are needed.

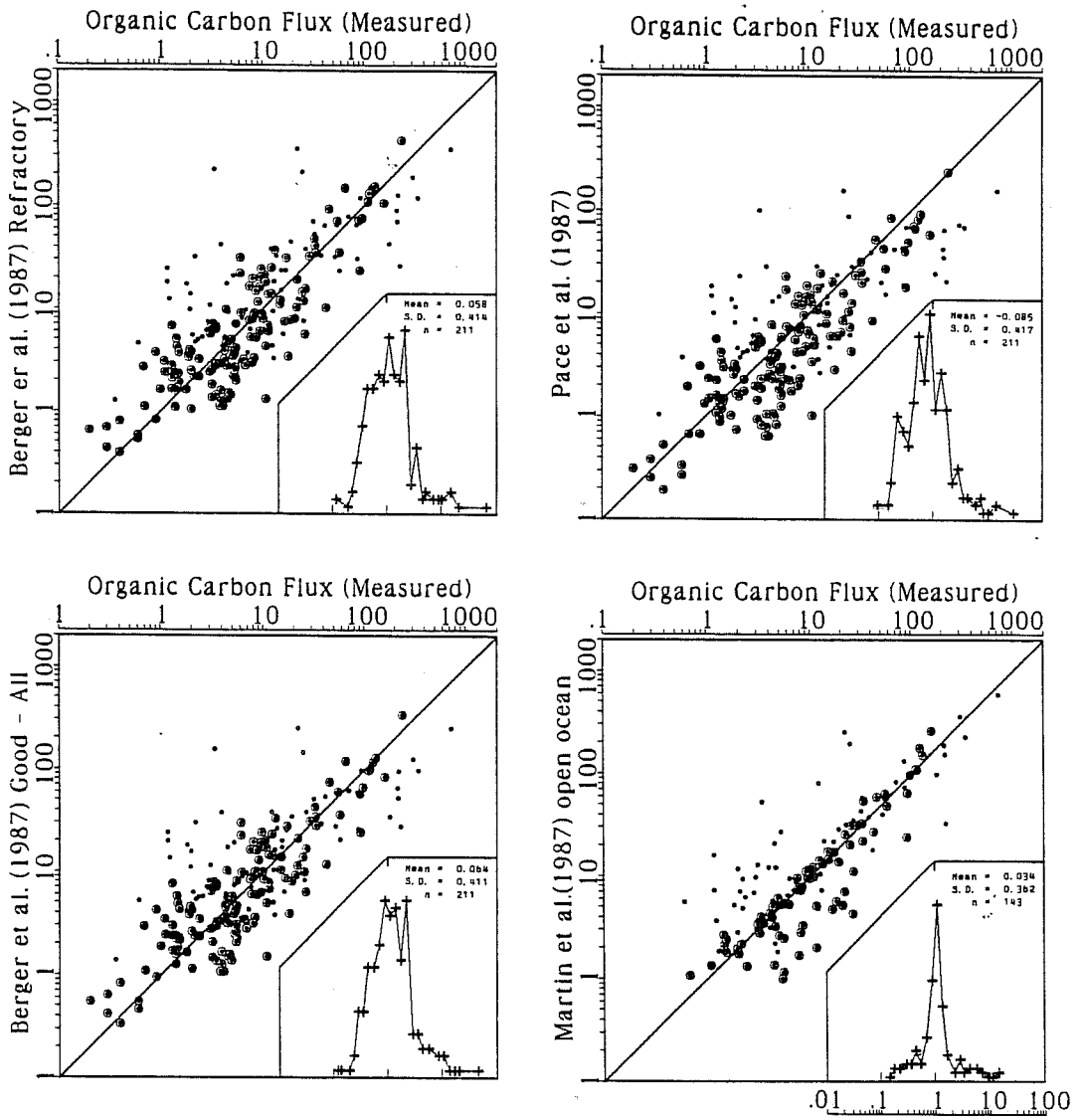

Fig. 3*b*—Test of empirical relationships (5–7) for carbon flux as a function of primary productivity and depth. Also a test of relationship (8) relating particle flux to known particle flux at 100 m depth. It is clear that knowing the particle flux at 100 m allows a much improved estimation of deeper data at the same station than using primary productivity. One would naturally expect this since flux at one depth is used to calculate flux at greater depths. The y axis scales for the inset are 0–30 for all except (8), where the scale is 0–50.

NITROGEN AND PHOSPHORUS

No maps of global nitrogen and phosphorus fixation appear to be available. It is reasonable to use typical Redfield ratios for conversion between carbon and nitrogen units. Nitrogen measurements are frequently made along with carbon measurements and no great problems appear to exist. An empirical

relationship similar to Eq. 7 has been derived to predict nitrogen flux as a function of primary production and depth (Pace et al. 1987).

Phosphorus is a problem. Experimental and field evidence shows that phosphorus is preferentially released from particles relative to nitrogen and carbon (e.g., Bishop et al. 1977; Martin et al. 1979). Once below the euphotic zone, the large particles sampled by traps and pumps exhibit C/P ratios greatly exceeding the 106:1 Redfield ratio. Some reported ratios exceeded 1000:1. On the other hand, small particles filtered from seawater at the same depth frequently show ratios much closer to the Redfield ratio (Bishop et al. 1987). Either there is a methodological bias, or another mechanism apart from the vertical transport of phosphorus in large sinking particles gives the ocean its dissolved phosphate distribution.

SILICA

Global Distributions of Silica Productivity

Although dissolved Si has been extensively measured in the ocean, there have been few attempts to model the global silica cycle. Some still regard Si as having a deep regenerative cycle since profiles of this element frequently show continued increase into the bottom. The work of Berger (1968), Hurd (1972), and Nelson and Goering (1977) provide field and laboratory evidence for shallow silica dissolution. The high deep values for silica in the Pacific may be more related to the fact that the element is dominantly fixed by diatoms living in cold polar and subpolar waters. Such patterns of production are illustrated by Lisitzin (1972; Fig. 4), who used a global primary production map similar to that shown in Fig. 2 and his knowledge of the C/Si ratios of particulate matter filtered continuously from near surface waters during cruises.

Vertical Fluxes of Silica

Little or no sediment trap data exists on the Si flux profiles from the euphotic zone to 1000 m. The few sediment trap data published usually include a single sample within this depth interval. LVFS data from the Panama Basin indicate strong Si dissolution in the upper 1000 m.

CARBONATE

Global Estimates of Carbonate Productivity

According to Lisitzin (1972), the global distributions of coccolith and foraminiferal productivity are maximal between 50°N and 50°S and generally

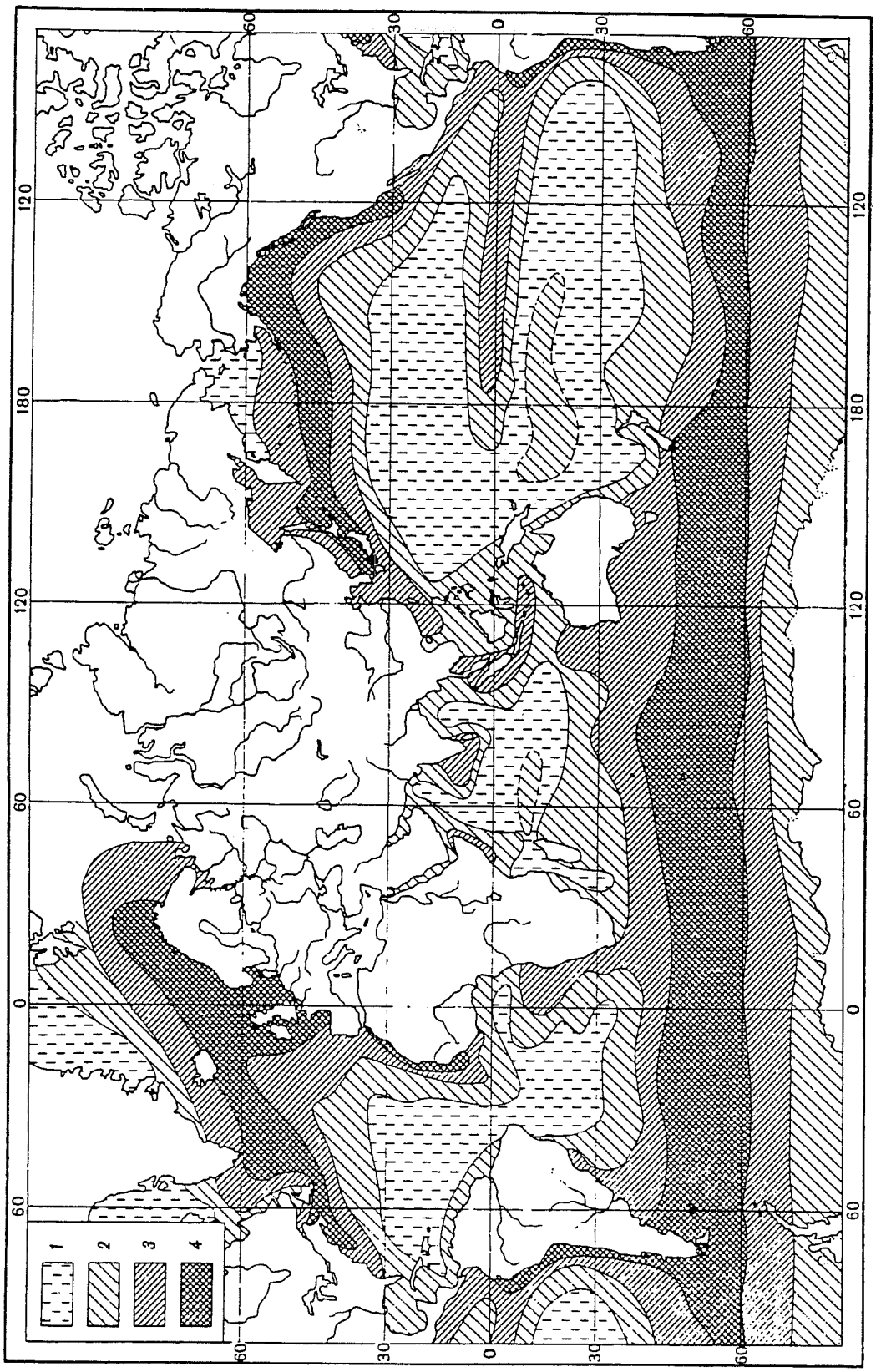

Fig. 4—Annual production of opaline silica in the world ocean (g SiO_2 $m^{-2}y^{-1}$) (from Lisitzin 1972). Key: 1 = <100; 2 = 100–250; 3 = 250–500; 4 = >500. The cross-hatched area centered at 15°S and 180°W is from a printing error in early primary productivity maps and should be <100 (see Berger et al. 1987, p. 49).

coincide with waters warmer than 10°C. His analysis of suspended carbonate distributions in surface waters showed highest concentrations near the Antarctic convergence in the southern hemisphere from 40–60°S, near the polar front in the northern hemisphere, and along the continental margins. Concentrations in equatorial zones were higher than in the gyres. No maps of global carbonate productivity have been drawn.

Vertical Fluxes of Carbonate

There has been no attempt to derive empirical relationships relating vertical fluxes of carbonate to primary productivity. As for silica, few sediment trap data are reported for carbonate flux in shallow waters. The most comprehensive data on fluxes which are published (Betzer, Byrne et al. 1984) appear to be severely biased by entrapment of living pteropods (Harbison and Gilmer 1986). Estimates from LVFS deployments suggest that shallow dissolution of carbonate (especially coccolith carbonate) is a typical occurrence in the eastern equatorial Pacific. This appears to occur in spite of the fact that the water column is supersaturated with respect to calcite from the surface to 1000–2000 m (Bishop et al. 1980, 1987). Evidence for shallow carbonate dissolution in the supersaturated waters of the Atlantic thermocline has been presented by Takahashi et al. (1985). Foraminifera shells have the greatest chance to reach the seafloor unaltered since their residence time in the water column is on the order of days and there is no food value in their empty shells. Foraminifera fluxes may vary by orders of magnitude over time scales of days in productive waters (Bé et al. 1985).

EMPIRICAL SOURCE FUNCTION MAPS FOR ORGANIC CARBON, OPAL, CARBONATE, AND BARIUM

The above sections have focused mainly on rate measurements and empirically derived relationships for estimating particulate carbon flux. This section was motivated by the simple rules suggested by Lisitzin (1972, for carbonate and opal) and most recently by Berger et al. (1987, for organic carbon). All suggested that abundances of particulate matter (and hence patterns of production) could be specified by simple transforms between a well measured quantity (ocean temperature, ocean nutrients, light) and the mean abundances of chemical species in suspended particulate matter. This work was also motivated by evidence suggesting that suspended barium concentrations (which frequently showed maxima at several hundred meters) could be used as an index of organic matter regeneration intensity (Bishop 1988). It must be stressed that parts of this section are speculative, but are deliberately so in order to promote discussion.

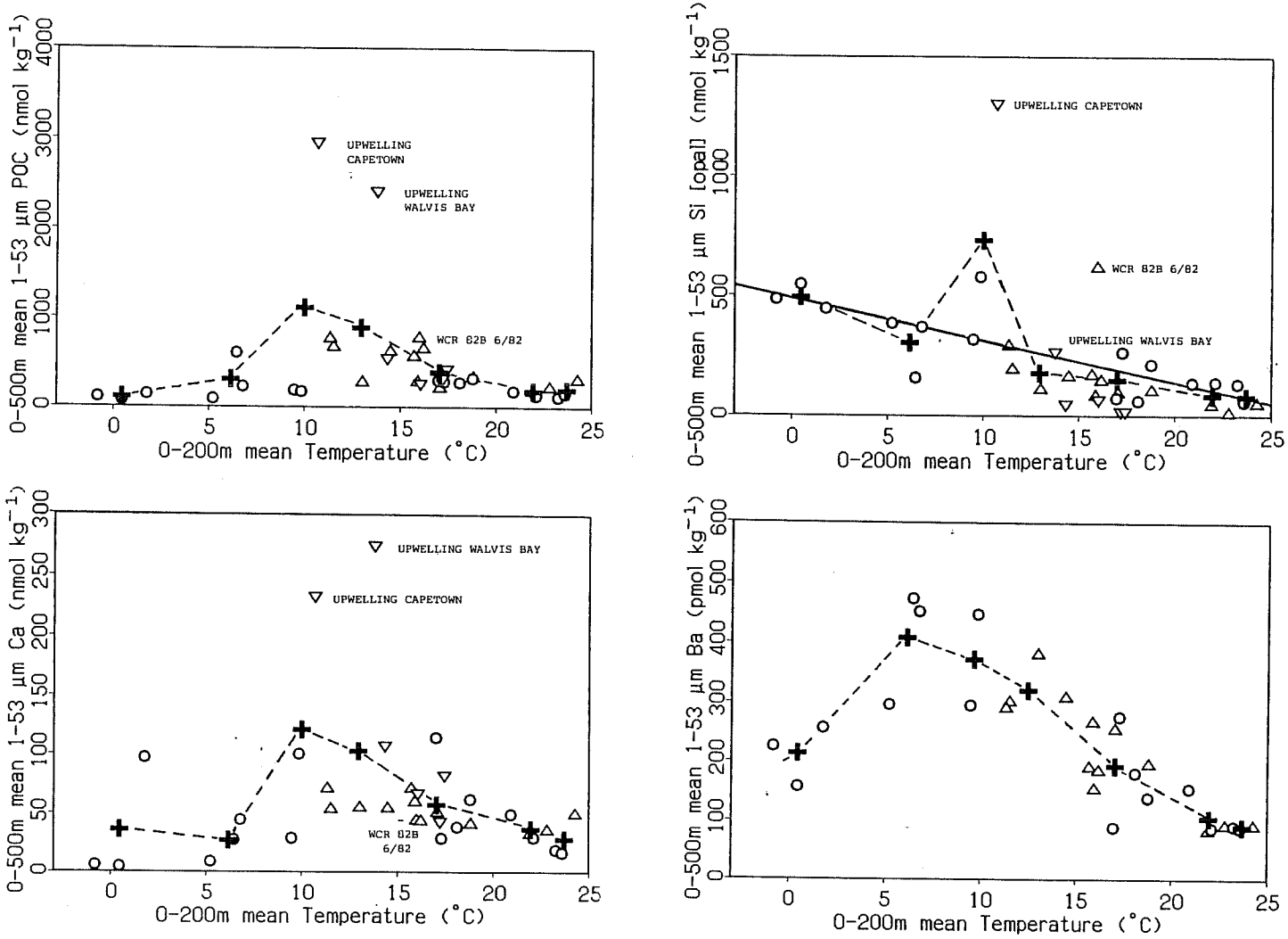

Fig. 5—Average particulate organic carbon, calcium carbonate, opal, and barium in the upper 500 m vs. mean water column temperature at 0–200 m. The (+) symbols denote averages used to derive maps 7–10 from map 6. ○ = GEOSECS data; ▽ = LVFS data from S.E. Atlantic; △ = LVFS data from N.W. Atlantic.

Data used in this analysis came from three sources: (*a*) unpublished Atlantic GEOSECS particulate matter data of Spencer and Brewer, (*b*) LVFS data from the N.W. Atlantic obtained as part of the Warm Core Rings Experiment, and (*c*) LVFS data from the S.E. Atlantic. Only the 1–53 μm LVFS data are used since the GEOSECS samples (10 liter volumes filtered through 0.4 μm Nucleopore filters) and 1–53 μm LVFS data (up to 25,000 liter volumes of water filtered through 1 μm glass or microquartz fiber filters) have been shown to yield equivalent suspended mass concentrations and the GEOSECS data were biased against >53 μm particles. Without going into detail, each kind of data set was processed to yield an estimate of organic carbon, opal, carbonate, and barium and integrated to 500 m (the 500 m limit was chosen to be deep enough to encompass the subsurface barium maximum) and averages were calculated. The organic carbon and opal calculated from GEOSECS chemical data had to be estimated from iodine measurements and gravimetric differences, respectively.

Temperature is inversely related to nutrient concentration in the upper ocean and therefore can be used as an index of nutrient concentration (Kamykowski and Zentara 1986). Profiles determined at each station were integrated to 200 m and the mean temperature calculated. The rationale for the 200 m limit was to be deep enough to minimize the effects of seasonal warming and cooling and yet to be shallow enough so as to adequately proxy nutrient availability to the euphotic zone. Testing other limits of integration yielded less satisfactory results when compared with the suspended matter data.

Figure 5 shows the results of such a correlation exercise. Barium showed a consistent relationship with temperature both in the GEOSECS data and WCRE data with maximum concentrations at 6°C. Silica increased with decreasing temperature. Superimposed on this increase were high values in some upwelling situations. Calcium carbonate and organic carbon tended to peak at intermediate temperatures. Consistently low concentrations for all elements were found in warmest waters. Means and standard deviations were calculated for the data partitioned in 4 degree temperature intervals.

Annual mean ocean temperature data from Levitus (1982) between 100°W and 20°E were used to calculate 0–200 m average temperatures for the Atlantic Ocean (Fig. 6). The empirical relationship relating the mean concentration and variability (standard deviation) of each element to temperature was used to generate corresponding maps (Figs. 7–10).

One question has been asked about the meaning of such maps constructed from few data points. It was suggested that the high values from upwelling situations might be eliminated since they appear to cause a bias of mapped distributions. The answer is that there is no rationale for eliminating particular points. For example, two data points from the S.E. Atlantic

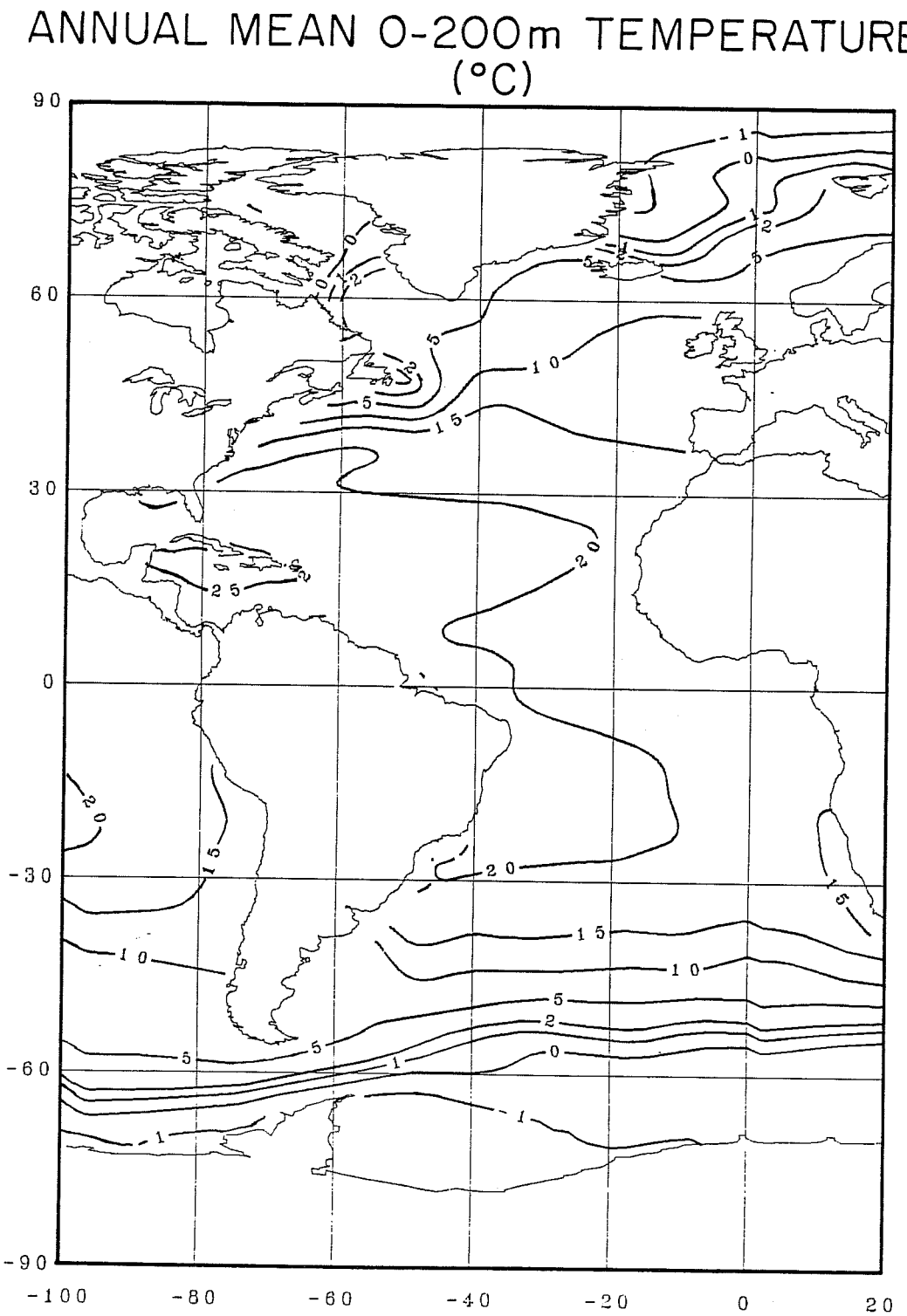

Fig. 6—Annual average 0–200 m ocean temperature (from Levitus et al. 1982).

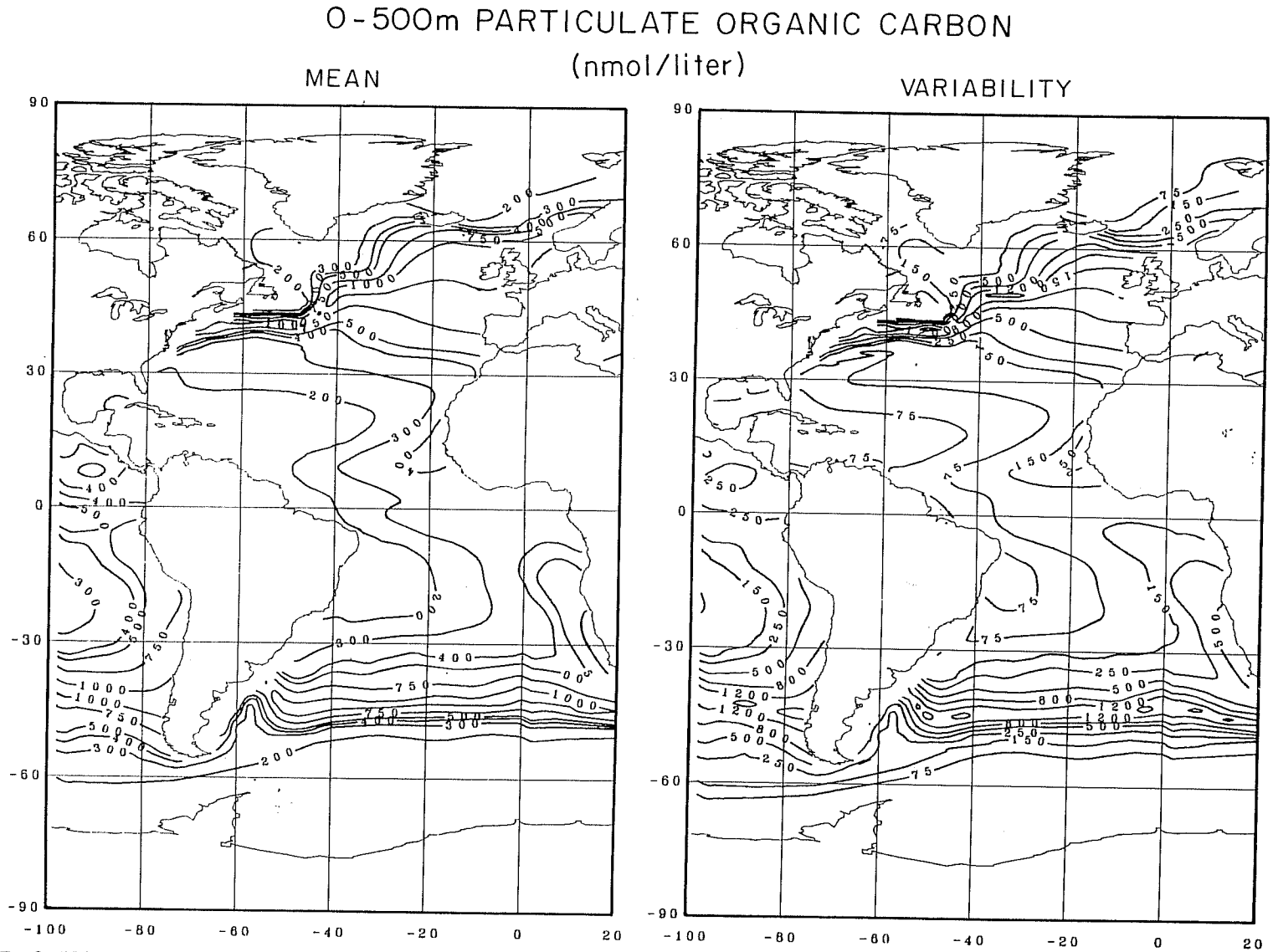

Fig. 7—0–500 m Particulate organic carbon. The left panel displays tne mean concentration derived from ocean temperature (Fig. 6). The right panel is a map of variability (standard deviation) of the data observations about the mean. Lowest concentrations are found in the warmest waters.

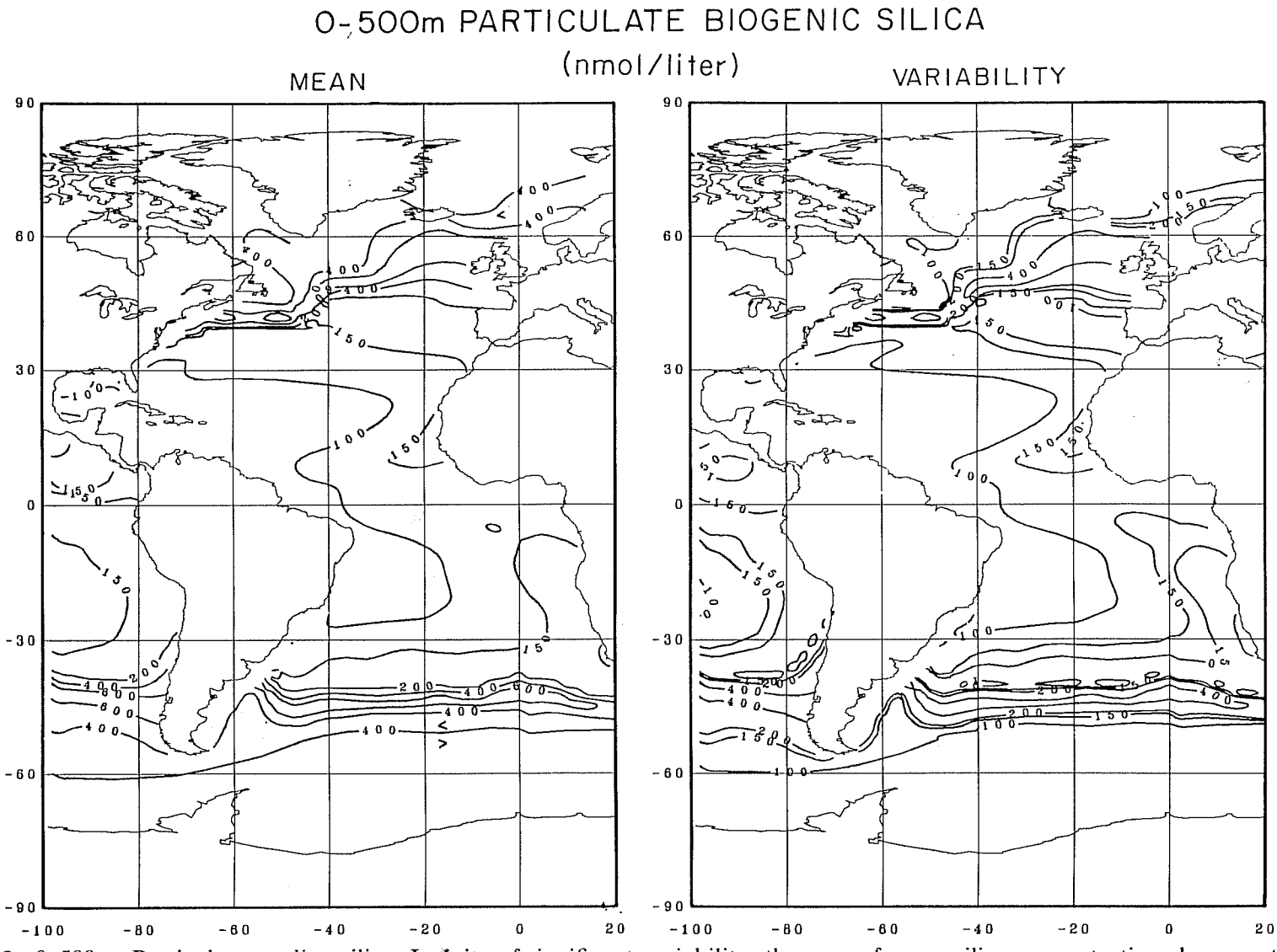

Fig. 8—0–500 m Particulate opaline silica. In spite of significant variability, the map of mean silica concentration shows a striking resemblance to the map of silica productivity drawn by Lisitzin (1972). Highest concentrations appear to occur in the subpolar waters south of Iceland and in the Southern Ocean.

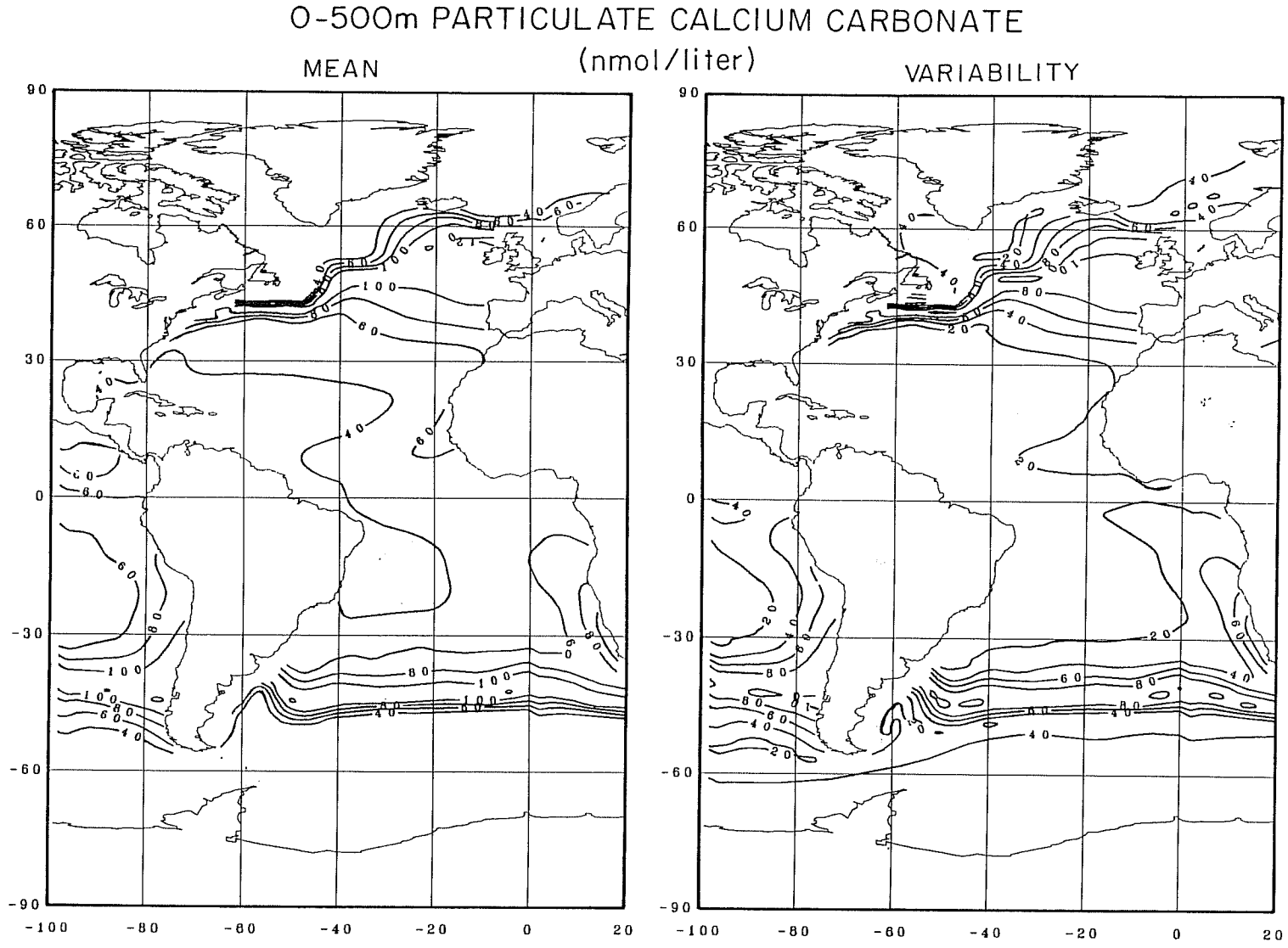

Fig. 9—0–500 m Particulate calcium carbonate. Distributions are highest in waters warmer than 10°C.

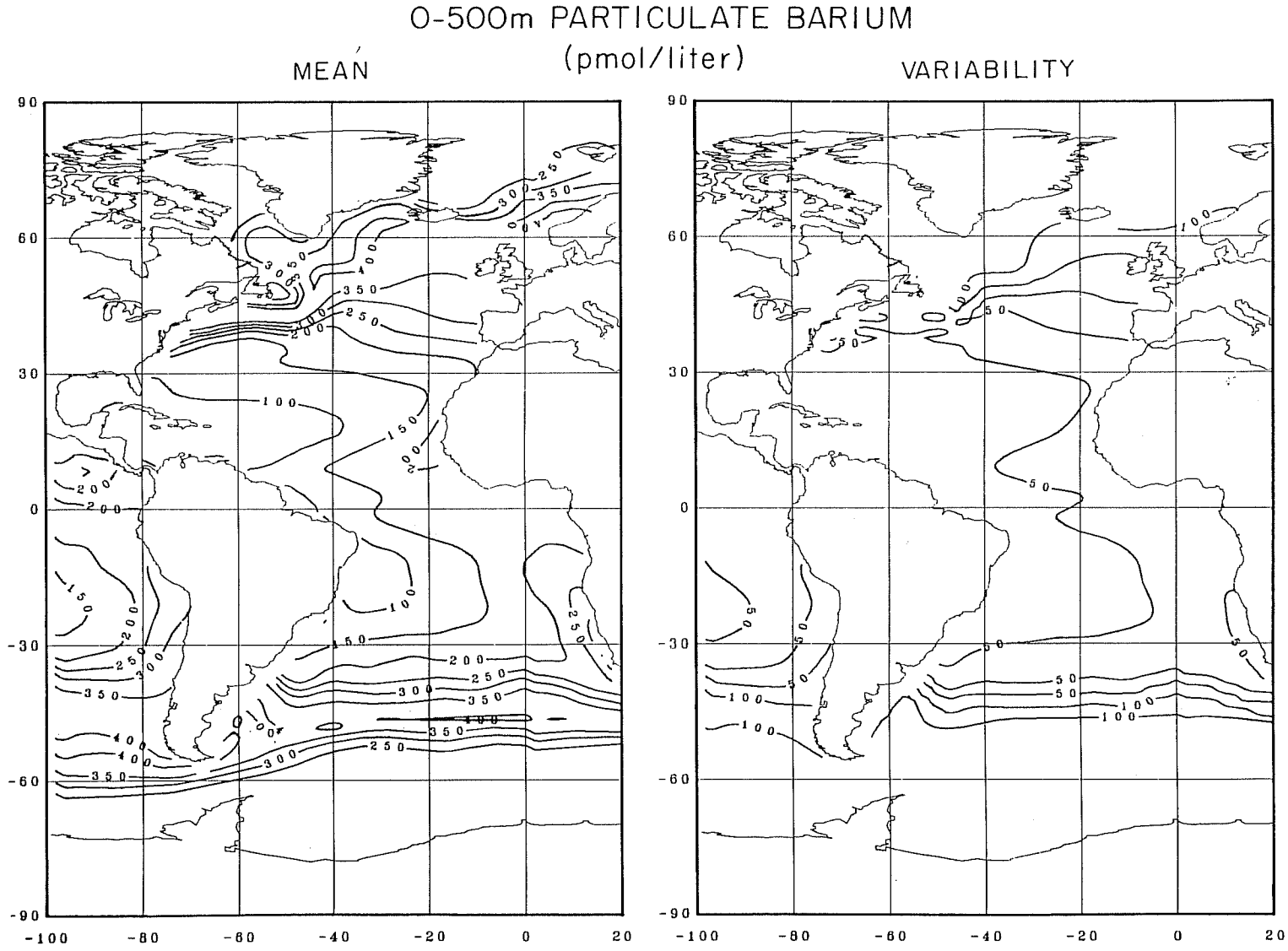

Fig. 10—0–500 m Particulate barium. The distributions of this element show the least variability of all variables mapped and Ba appears to be a good indicator of ocean regions with intense organic production.

appear to be anomalous in carbon and calcium but only one is anomalous in silica. One point anomalous in Si was not anomalous in Ba, Ca, or organic carbon. The important point of this exercise is to illustrate that the suspended particulate matter field does correlate with distributions of ocean physical properties and this information can be used to derive first-order patterns for the production function of each element. By considering the variability as well, we can map regions of the ocean which may contain great variability.

The striking feature of these maps is that the features of the carbon, opal, and carbonate fields reflect closely features described in the previous section. Carbon distributions reflect upwelling and ocean frontal regions. For example, productive regions in the eastern equatorial Pacific (Peru upwelling, Costa Rica Dome) are resolved. Carbonate patterns are confined mostly between 50°N and 50°S and are maximal in the subpolar regions consistent with Lisitzin's simple rule. Some variability may occur in polar waters. Opal patterns are strongest in subpolar zones, remain high in polar regions, and correspond closely with Fig. 4. Barium dominates subpolar and upwelling regions, perhaps indicating global patterns of organic matter regeneration intensity. The warm gyres of the North and South Atlantic contain lowest amounts of all quantities.

Maps of variability (with the exception of barium) show maximal values in the subpolar regions and gyre boundaries. These regions may be naturally variable and therefore may be important areas for the transfer of chemically reactive particles into the deep sea. The regions of great variability are regions of the ocean where more work is required to understand the nature of the variability.

The maps illustrate how knowledge of the suspended particle field leads to simple empirical rules for inferring the production patterns of organic matter, carbonate, opal, and barium. Understanding the workings of the biological pump in the subpolar, frontal, and upwelling regions will be needed to fully evaluate patterns of ocean productivity past and present.

CONCLUSION

Simple rules may exist allowing us to specify the operation of the biological pump on a global basis. Clearly, there is a need to define more of the rules of operation of the pump through cross-disciplinary analysis of existing data and through new field work.

Acknowledgements. The author wishes to thank Drs Derek Spencer and Peter Brewer for providing access to their unpublished GEOSECS Atlantic particulate matter data. Drs W. Berger, P.E. Biscaye, S. Emerson, J. Marra, and V. Ittekkot are thanked for their reviews of the text. Sample collection

and analysis were supported by NSF grants OCE88-02773 and OCE85-13420 and ONR contract N00014-80-C-0098. This effort was supported by the NASA cooperative agreement NCC5-29A to Columbia University. L-DGO contribution number 4385.

REFERENCES

Bé, A.W.H.; Bishop, J.K.B.; Sverdlove, M.S.; and Gardner, W.D. 1985. Standing stock, vertical distribution and flux of planktonic foraminifera in the Panama Basin. *Mar. Micropal.* **9**: 307–333.

Berger, W.H. 1968. Radiolarian skeletons: solution at depths. *Science* **159**: 1237–1239.

Berger, W.H.; Fisher, K.; Lai, C.; and Wu. G. 1987. Ocean carbon flux: global maps of primary production and export production. In: Biogeochemical Cycling and Fluxes between the Deep Euphotic Zone and Other Oceanic Realms, ed. C. Agegian. NOAA Symp. Ser. for Undersea Research, NOAA Undersea Research Program, vol. 3(2). Preprint in SIO ref. 87–30.

Betzer, P.R.; Byrne, R.H.; Acker, J.G.; Lewis, C.S.; Jolley, R.R.; and Feely, R.A. 1984. The oceanic carbonate system: a reassessment of biogenic controls. *Science* **226**: 1074–1076.

Betzer, P.R.; Showers, W.J.; Laws, E.A.; Winn, C.D.; DiTullio, G.R.; and Kroopnick, P.M. 1984. Primary productivity and particle fluxes on a transect of the equator at 153 W in the Pacific Ocean. *Deep-Sea Res.* **31**: 1–12.

Bishop, J.K.B. 1988. The barite-opal-organic carbon association in oceanic particulate matter. *Nature* **233**: 241–243.

Bishop, J.K.B.; Collier, R.W.; Ketten, D.R.; and Edmond, J.M. 1980. The chemistry, biology and vertical flux of particulate matter from the upper 1500 m of the Panama Basin. *Deep-Sea Res.* **27**: 615–640.

Bishop, J.K.B.; Edmond, J.M.; Ketten, D.R.; Bacon, M.P.; and Silker, W.B. 1977. The chemistry, biology and vertical flux of particulate matter from the upper 400 m of the equatorial Atlantic ocean. *Deep-Sea Res.* **24**: 511–548.

Bishop, J.K.B.; Stepien, J.C.; and Wiebe, P.H. 1987. Particulate matter distributions, chemistry and flux in the Panama Basin: response to environmental forcing. *Prog. Ocean.* **17**: 1–59.

Bruland, K., and Coale, K.H. 1986. Surface water $^{234}Th/^{238}U$ disequilibria: spatial and temporal variations of scavenging rates within the Pacific Ocean. In: Dynamic Processes in the Chemistry of the Upper Ocean, eds. J.D. Burton, P.G. Brewer, and R. Chesselet, pp. 159–172. New York: Plenum.

Dugdale, R.C., and Goering, J.J. 1967. Uptake of new and regenerated forms of nitrogen in primary productivity. *Limnol. Ocean.* **12**: 196–206.

Harbison, G.R., and Gilmer, R.W. 1986. Effects of animal behavior on sediment trap collections: implications for the calculation of aragonite fluxes. *Deep-Sea Res.* **33**: 1017–1024.

Hurd, D.C. 1972. Factors affecting solution rate of biogenic opal in sea water. *Earth Planet. Sci. Lett.* **15**: 411–417.

Kamykowski, D. 1987. A preliminary biophysical model of the relationship between temperature and plant nutrients in the upper ocean. *Deep-Sea Res.* **34**: 1067–1079.

Kamykowski, D., and Zentara, S.-J. 1986. Predicting plant nutrient concentration from temperature and sigma-t in the world ocean. *Deep-Sea Res.* **33**: 89–105.

Koblentz-Mishke, O.J.; Volkovinsky, V.V.; and Kabanova, J.G. 1970. Plankton primary production of the world ocean. In: Scientific Exploration of the South

Pacific, ed. W.S. Wooster, pp. 183–193. Washington, D.C.: National Academy of Sciences.

Levitus, S. 1982. Climatological Atlas of the World Ocean. NOAA Prof. Paper 13, US Dept of Commerce.

Lisitzin, A.P. 1972. Sedimentation in the World Ocean. Spec. Publ. 17. Tulsa, OK: Soc. Econ. Paleon. Miner.

Martin, J.H.; Knauer, G.A.; and Bruland, K. 1979. Fluxes of particulate carbon, nitrogen, and phosphorus in the upper water column of the northeast Pacific. *Deep-Sea Res.* **26**: 97–108.

Martin, J.H.; Knauer, G.A.; Karl, D.M.; and Broenkow, W.W. 1987. VERTEX: carbon cycling in the northeast Pacific. *Deep-Sea Res.* **34**: 267–286.

Nelson, D.M., and Goering, J.J. 1977. Near-surface silica dissolution in the upwelling region off northwest Africa. *Deep-Sea Res.* **24**: 31–36.

Pace, M.L.; Knauer, G.A.; Karl, D.M.; and Martin, J.M. 1987. Primary production, new production and vertical flux in the eastern Pacific Ocean. *Nature* **325**: 803–804.

Suess, E. 1980. Particulate organic carbon flux in the ocean—surface productivity and oxygen utilization. *Nature* **288**: 260–263.

Takahashi, T.; Broecker, W.S.; and Langer, S. 1985. Redfield ratio based on chemical data from isopycnal surfaces. *J. Geophys. Res.* **90**: 6907–6924.